Environmental Science & Technology

pubs.acs.org/est

Article

Fire Impacts on the Soil Metabolome and Organic Matter Biodegradability

Jacob P. VanderRoest, Julie A. Fowler, Charles C. Rhoades, Holly K. Roth, Corey D. Broeckling, Timothy S. Fegel, Amy M. McKenna, Emily K. Bechtold, Claudia M. Boot, Michael J. Wilkins, and Thomas Borch*

Cite This: *Environ. Sci. Technol.* 2024, 58, 4167−4180

Read Online

ACCESS | Metrics & More | Article Recommendations | Supporting Information

ABSTRACT: Global wildfire activity has increased since the 1970s and is projected to intensify throughout the 21st century. Wildfires change the composition and biodegradability of soil organic matter (SOM) which contains nutrients that fuel microbial metabolism. Though persistent forms of SOM often increase postfire, the response of more biodegradable SOM remains unclear. Here we simulated severe wildfires through a controlled "pyrocosm" approach to identify biodegradable sources of SOM and characterize the soil metabolome immediately postfire. Using microbial amplicon (16S/ITS) sequencing and gas chromatography−mass spectrometry, heterotrophic microbes (*Actinobacteria, Firmicutes,* and *Protobacteria*) and specific metabolites (glycine, protocatechuate, citric cycle intermediates) were enriched in burned soils, indicating that burned soils contain a variety of substrates that support microbial metabolism. Molecular formulas assigned by 21 T Fourier transform ion cyclotron resonance mass spectrometry showed that SOM in burned soil was lower in molecular weight and featured 20 to 43% more nitrogen-containing molecular formulas than unburned soil. We also measured higher water extractable organic carbon concentrations and higher CO_2 efflux in burned soils. The observed enrichment of biodegradable SOM and microbial heterotrophs demonstrates the resilience of these soils to severe burning, providing important implications for postfire soil microbial and plant recolonization and ecosystem recovery.

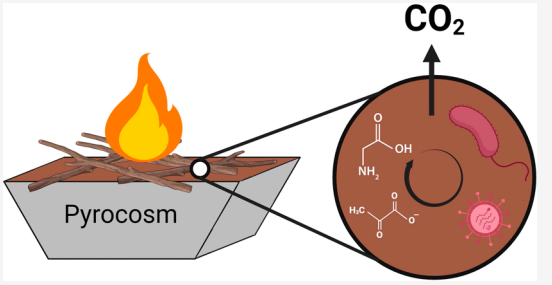

INTRODUCTION

Wildfires are widespread ecosystem disturbances that burn millions of hectares each year and are beneficial within fire-adapted environments.[1−4] However, over the past five decades, wildfires have become more frequent, severe (i.e., more vegetation and organic matter are consumed during burning), intense (i.e., higher temperatures and energy output), and are projected to increase in size.[5−8] Thus, understanding how wildfires impact terrestrial ecosystems and the soils that support them is essential.

Wildfires change the composition of both soil organic matter (SOM) (a heterogeneous mixture of organic molecules ranging from low-molecular weight metabolites to lignin-like, proteinaceous, and humic-like substrates) and the soil microbiome (an assemblage of archaea, bacteria, fungi, and viruses).[9] SOM serves as carbon and energy sources for microbes, and microbial metabolism of SOM depends on SOM composition.[10] Wildfires disrupt the interplay between SOM and microbial communities by reducing soil microbial biomass,[11] decreasing microbial Shannon's diversity,[12] shifting microbial community composition (e.g., enrichment in *Actinobacteria* and loss of ectomycorrhizal fungi)[12,13] and function (e.g., increased thermotolerance and aromatic organic matter degradation),[12,14−17] altering soil mycorrhizal-plant associations,[13] and changing SOM composition.[9,12,18−21] Therefore, studying linkages between postfire SOM composition and microbial community structure is essential to understand the extent that microbes metabolize SOM in burned soils to fuel postfire microbial recolonization and soil recovery.

Extensive work has evaluated the impact of wildfires on SOM and the formation, composition, and reactivity of pyrogenic organic matter (PyOM), which is thermochemically altered organic matter.[9,18,21−36] PyOM can be highly resistant to biological degradation compared to unburned OM, with half-lives ranging over millennial time scales (~500 to 8000 years).[23,37] However, recent review papers and laboratory studies indicate that PyOM can exhibit varying degrees of biodegradability with certain carbon pools featuring half-lives of a few weeks to months.[22,33,38] Fischer et al. observed PyOM metabolism by incubating fungi with ^{13}C-labeled burned pine wood for 57 days and detected the release of respired ^{13}C-

Received: November 22, 2023
Revised: February 5, 2024
Accepted: February 9, 2024
Published: February 22, 2024

https://doi.org/10.1021/acs.est.3c09797
Environ. Sci. Technol. 2024, 58, 4167−4180

labeled CO_2.[39] Goranov et al. and Bostick et al. conducted incubations of aqueous extracts of burned oak wood with soil-extracted microbes and, respectively, observed a 16% decrease in C content and a 25 to 67% decrease in aromatic content after only 10 days.[40,41] These studies demonstrate rapid PyOM metabolism that includes aromatic substrates previously considered highly resistant to biodegradation.[39,41] However, laboratory studies have not historically accounted for the polyfunctionality, polydispersity, and molecular complexity of soils, soil carbon, and environmental factors that influence SOM biodegradation (e.g., organo-mineral interactions, soil redox conditions).[42−44] Therefore, it is necessary to evaluate 1) if the biodegradability of laboratory-produced PyOM accurately represents SOM biodegradability in wildfire-burned soils and 2) what biochemical mechanisms drive PyOM degradation.

Prior studies propose mechanisms for aromatic SOM biodegradation in burned soils, but those mechanisms have not been confirmed with chemical analyses such as mass spectrometry.[12,39] Fischer et al. and Nelson et al. observed the expression of genes associated with the degradation of aromatic molecules within microbial communities that were either incubated with pyrogenic carbon or collected from wildfire-burned soils.[12,39] Both studies independently proposed pathways that generate two key intermediate compounds: catechol and protocatechuate.[12,39] The proposed end products of the degradation are the coenzymes succinyl-CoA and acetyl-CoA, which feed into the citric acid cycle: a central metabolic pathway that releases stored energy from carbohydrates, fats, and proteins, fueling microbial activity.[12,39] These proposed pathways suggest that PyOM, which can remain stable for centuries, can also be metabolized and transformed into metabolites that funnel into key metabolic pathways. However, the proposed pathways were inferred based only on the presence and expression of genes associated with aromatic compound degradation. With the exception of catechol, no other intermediates in these pathways have been detected in burned soils.[45] Moreover, detailed metabolomics analysis of SOM from burned soils has not yet been conducted, so the relative abundance of low-molecular weight metabolites (e.g., saccharides, organic acids, and amino acids) in burned soils remains unknown.

Mass spectrometry can address these knowledge gaps by detecting metabolites and determining broader SOM composition. Pyrolysis gas chromatography−mass spectrometry (GC-MS) has been used to detect low molecular weight molecules in burned soils to examine general changes in postfire SOM composition rather than determining shifts in metabolite content related to microbial metabolism.[46−51] Therefore, GC-MS, which can target specific molecules (targeted analysis) and annotate detected peaks (nontargeted analysis), could be used to elucidate the unknown pools of metabolites in burned soils that likely interact with active microbial assemblages.[52,53] While ideal for detecting specific metabolites, GC-MS features relatively low mass resolution and mass accuracy, limiting its ability to evaluate SOM composition broadly. Fourier transform ion cyclotron resonance mass spectrometry (FT-ICR MS) has high mass resolving power (up to 3,000,000 at m/z 200), high accuracy (subppm mass measurement error), and assigns molecular formulas across a wide mass range (175−1200 Da).[54] Due to the complexity of SOM, FT-ICR MS is an ideal technique for elucidating SOM composition broadly to compensate for the resolution limitations of GC-MS.[12,18,19,24,55,56]

We simulated a wildfire using a controlled pyrocosm approach[57] to elucidate SOM composition changes associated with microbial activity in burned soil. The objectives were to 1) characterize SOM and microbial community composition throughout the first month following fire, 2) identify postfire shifts in the soil metabolome and metabolite abundances, and 3) determine how changes in SOM composition correspond to microbial community structure. We hypothesized that 1) soil microbes present immediately after burning would mineralize SOM and release CO_2 and that 2) intermediate metabolites in aromatic degradation pathways—namely, catechol, protocatechuate, and citric acid cycle metabolites—would be enriched in burned soil.[12,39] We addressed these objectives and hypotheses by characterizing SOM composition at the molecular level with GC-MS and FT-ICR MS and by characterizing soil microbiome composition using16S rRNA gene and ITS amplicon sequencing.

MATERIALS AND METHODS

Pyrocosm Preparation and Burning. Mineral soil and forest litter were collected in August 2022 from an unburned portion of a lodgepole-pine-dominated (*Pinus contorta*) forest located along Long Draw Road near Cameron Pass, Colorado (40° 30' 55.4400" N and 105° 46' 4.9080" W) with an approximate elevation of 3050 m.[58] Total annual precipitation averages 783 mm, and mean annual temperature is 1.1 °C with average annual minima and maxima of −6.4 °C and 8.8 °C, respectively.[58] This location is representative of a subalpine forest that is burned by wildfires. After removing the litter layer and O-horizon, mineral soil was collected at a depth of 0−10 cm, sieved to 4 mm sieve, homogenized by mixing, and added into pyrocosms.

Pyrocosms simulate a wildfire burn and provide control over experimental variables (e.g., soil type, fuel type, burn duration).[57] The pyrocosms were 53 L galvanized steel buckets (56 cm in length, 25 cm in height, and 38 cm in width) with holes (0.56 cm diameter) drilled into the sides of the pyrocosm (Figure S1). K-type thermocouples (Extech Instruments) were inserted at depths of 1, 5, 8, and 12 cm below the mineral soil surface for three pyrocosms that were going to be burned labeled "B1," "B2," and "B3" ("B" representing burned). The tips of the thermocouples reached the central area of the B1, B2, and B3 pyrocosms. Three control pyrocosms were labeled "UB1," "UB2," and "UB3" ("UB" representing unburned).

The pyrocosms were transported to the Colorado State University Agricultural Research, Development, and Education Center (ARDEC). The B1, B2, and B3 pyrocosms were dug 4.5 m apart to a depth at which the mineral soil inside the pyrocosms was level with the surrounding soil. The UB1, UB2, and UB3 pyrocosms were positioned approximately 30 m away from the B1, B2, and B3 pyrocosms. The collected forest litter was added on top of all six pyrocosms to a depth of approximately 2 cm. The average gravimetric water content of the six pyrocosms prior to burning was 8.6 ± 1.1%.

Approximately 21 kg of lodgepole pine wood was burned on each of the B1, B2, and B3 pyrocosms (Figure S2), and soil temperature was monitored during burning (Figure S3). The measured temperatures were representative of a high intensity wildfire.[59] No wood was burned on top of the UB1, UB2, or UB3 pyrocosms. The morning after the burns (referred to as "Day 0"), a soil density core (6 cm diameter, 10 cm height)

https://doi.org/10.1021/acs.est.3c09797
Environ. Sci. Technol. 2024, 58, 4167−4180

was inserted into each of the six pyrocosms. The ash layer in the core was discarded for B1, B2, and B3, and the forest litter layer in the core was discarded for UB1, UB2, and UB3. Mineral soil was sampled from the core to a depth of 0−5 cm. Next, 2 L of Milli-Q water (18 MΩ cm) was added to all pyrocosms to simulate a 1.27 cm precipitation event which falls within the range of precipitation events occurring within Cameron Pass.[58] No additional water was deliberately added to the pyrocosms. Limited natural precipitation events did occur during the soil sampling period (see Figure S4 for precipitation details).[60]

Mineral soil samples (0−5 cm) were collected 3 days ("Day 3"), 7 days ("Day 7"), 14 days ("Day 14"), and 28 days ("Day 28") after the burn event, generating a total of 30 mineral soil samples for the entire study that were stored in zip-top bags in a fridge at 4 °C (Figure S4). Subsamples of all 30 soil samples were stored in sterile Whirlpak bags (Uline, Pleasant Prairie, WI, USA) in a −80 °C freezer for later microbial analyses. During this 28-day sampling period, the pyrocosms were left at ARDEC and were not disturbed or covered. This 28-day sampling period was selected due to the paucity of studies examining immediate postfire alterations to SOM and soil microbes whereas studies sampling soil multiple months and years postfire are comparatively common (see in Section 2 of the Supporting Information for more rationale for using pyrocosms).[12,13,18,24,55,61,62] See Table S1 for a summary of the analytical techniques employed for each soil sample.

Total Soil Carbon and Nitrogen. Air-dried, 2-mm sieved mineral soil was ground and sieved through a 125-μm sieve. Total carbon and total nitrogen were measured using a Carbon Nitrogen Analyzer (VELP Scientifica CN 802, Deer Park, NY, USA).

Soil pH. For each soil sample, 20 g of air-dried (24 h at room temperature), 2-mm sieved mineral soil was shaken with 40 mL of Milli-Q water for 1 h. A Thermo Scientific Orion Star A215 pH/conductivity meter and a Thermo Scientific Orion Double Junction pH probe were calibrated with VWR pH reference standards, and the pH electrode was inserted into the soil-water slurry after shaking the soil slurry by hand to resuspend the soil. Then, 2 mL of a 0.21 M solution of $CaCl_2$ (Fisher Chemical) was added to each sample to produce a final concentration of 0.01 M $CaCl_2$. These soil-water slurries were shaken by hand, and pH was measured.

Water-Extractable Organic Carbon and Water-Extractable Total Nitrogen. For each soil sample, 20 g of air-dried (24 h at room temperature), 2-mm sieved soil, and 100 mL of Milli-Q water was shaken for 1 h at 200 rpm. The supernatant from each sample was then filtered through 0.45 μm glass fiber filter (Advantec MFS, Inc.). Dissolved organic carbon and dissolved total nitrogen for each sample were measured using a TOC-L Shimadzu analyzer (Shimadzu Corporation, Columbia, MD, USA). The measured dissolved organic carbon and dissolved total nitrogen mass were then normalized to the mass of soil to calculate water-extractable organic carbon and water-extractable total nitrogen, respectively.

Ammonium. For each soil sample, 10 g of air-dried, 2-mm sieved mineral soil was shaken with 50 mL of 2 M KCl for 1 h followed by filtration through alpha cotton cellulose filter paper (Whatman plc). Ammonium concentrations were measured using a flow injection analyzer (Lachat QuikChem, 8500, Hach Scientific, Loveland, CO).

Gas Chromatography−Mass Spectrometry (GC-MS). Soil-water extracts were filtered, derivatized via methoximation and silylation, and analyzed with an electron impact, Thermo Trace 1310 GC coupled with ISQ single quadruple MS with liquid autosampler. Section 3 of the Supporting Information includes descriptions of soil-water extractions, GC-MS operating conditions, and data processing. Peak areas were normalized with total ion current normalization, and annotations were assigned by comparing fragmentation spectra to library databases. Standards for catechol (Sigma-Aldrich, >99% purity) and protocatechuate (Sigma-Aldrich, >97% purity) were used for targeted analysis.

Twenty-One Tesla Fourier Transform Ion Cyclotron Resonance Mass Spectrometry (FT-ICR MS). After shaking 50 g of air-dried, 2-mm sieved mineral soil with 100 mL of Milli-Q water for 19 h at 170 rpm, each soil-water extract was filtered (0.22 μm poly(ether sulfone) membrane, Merck Millipore Ltd.). The SOM was concentrated with solid-phase extraction (Agilent Bond Elut PPL [Priority Pollutant] styrene-divinylbenzene polymer cartridges) and infused via a micro-electrospray ionization (ESI) source operating in negative and positive modes.[63] SOM extracts were analyzed with a custom-built hybrid linear ion trap FT-ICR mass spectrometer equipped with a 21 T superconducting solenoid magnet.[64,65] Mass spectra were phase-corrected and internally calibrated with 10−15 highly abundant homologous series that span the entire molecular weight distribution based on the "walking" calibration method.[66,67] Using PetroOrg© software, experimentally measured masses were converted to the Kendrick mass scale[68] to identify homologous series for each heteroatom class (specifically KMD_{CH2} for molecules differing only by degree of alkylation),[69] and molecular formulas containing carbon (C), hydrogen (H), oxygen (O), nitrogen (N), and sulfur (S) were assigned using the experimentally measured masses.[70−73] Molecular formula assignments with a mass error >0.35 parts-per-million were discarded. For all mass spectra presented herein, between 9,891 and 21,150 peaks were assigned elemental compositions with root-mean-square mass measurement accuracy of 26 to 36 ppb with an average achieved resolving power of 3,400,000 at m/z 200. Tables S2 and S3 show the number of assignments and average root-mean-square (RMS) error for all assigned species present in this publication. All 21 T FT-ICR MS files and elemental composition assignments are publicly available via the Open Science Framework at DOI 10.17605/OSF.IO/PB8QU (https://osf.io/pb8qu/). Section 4 of the Supporting Information includes further descriptions of the soil-water extractions, solid phase extraction, and FT-ICR MS operating conditions and data processing procedure.

Soil CO_2 Respiration Incubations. Soil CO_2 respiration measurements were conducted with burned and unburned soil collected on Day 0, Day 14, and Day 28. The five replicates of Day 0, Day 14, and Day 28 burned and unburned soil samples were air-dried overnight, generating a total of 30 subsamples. For each subsample, approximately 20 g of air-dried soil and 6.7 mL of Milli-Q water were added to 120 mL plastic beakers. The beakers were placed individually in half-gallon jars with an airtight lid featuring a rubber septum and stored in the dark in a constant temperature room (25 °C).[74] CO_2 accumulation in the jar headspace was measured using an infrared gas analyzer (IRGA, model LI-6252, LICOR). After flushing the jars with CO_2-free air (prepared by passing compressed air through soda lime), a subsample of the jar headspace (1 to 10 mL) was

https://doi.org/10.1021/acs.est.3c09797
Environ. Sci. Technol. 2024, 58, 4167−4180

extracted using a syringe and injected into the gas analyzer, generating a baseline CO_2 measurement. During the next measurement, the measured CO_2 quantity in the jar headspace was subtracted by the prior CO_2 quantity to quantify CO_2 emitted between sampling points. The jars were then flushed with CO_2-free air to prevent the jars from becoming too concentrated with CO_2, and the baseline CO_2 quantity was measured. This was repeated each time a CO_2 measurement was made, and the accumulated CO_2 values were summed to calculate the total CO_2 emitted.

Microbial Analyses. *DNA Extraction and 16S rRNA Gene and ITS Amplicon Sequencing.* Genomic DNA was extracted from each soil sample using the DNeasy PowerMax Soil Kit followed by concentration using a vacuum centrifuge for the burned samples and the DNeasy PowerLyzer PowerSoil Kit (Qiagen) for unburned soils following the manufacturer's protocol. Each kit utilizes the same fundamental chemistry, but the PowerLyzer Kit uses only 0.25 g of input compared to 10 g used in the PowerMax kit providing detectable DNA extraction from low biomass samples. Amplicon libraries were prepared using a single step PCR. Soil bacterial and archaeal communities were amplified using the V4 region of the 16S rRNA gene with the primers 515F[75] (5′-AATGATACGGCGACCACCGAGATCTACACGCT XXXXXXXXXXXX TATGGTAATT GT GTGYCAGCMGCCGCGGTAA-3′, where this sequence includes the 5′ Illumina adapter, the Golay barcode, the forward primer pad, the forward primer linker, and the forward primer, respectively) and 806R (5′-CAAGCAGAAGACGGCATACGAGAT AGTCAGCCAG CC GGACTACNVGGGTWTCTAAT-3′, where this sequence includes the reverse compliment of the 3′ Illumina adapter, the reverse primer pad, the reverse primer linker, and the reverse primer, respectively).[76] Soil fungal communities were amplified using the first internal transcribed spacer (ITS1) of the rDNA with the primers ITS 1f (5′-AATGATACGGCGACCACCGAGATCTACAC GG CTTGGTCATTTAGAGGAAGTAA −3′, where this sequence includes the Illumina adapter, the forward primer linker, and the forward primer, respectively) and ITS2(5′-CAAGCAGAAGACGGCATACGAGAT NNNNNNNNNN CG GCTGCGTTCTTCATCGATGC-3′, where this sequence includes the reverse compliment of the 3′ Illumina adapter, the Golay barcode, the reverse primer linker, and the reverse primer, respectively).[77] All primers were modified to include Illumina adaptors and unique barcodes as done in the Earth Microbiome Project (EMP) (https://earthmicrobiome.org/).[78] The EMP PCR protocol was modified to use Platinum II Hot Start PCR Master Mix (Invitrogen). PCR products were normalized using SequalPrep Normalization Plate Kit (Applied Biosystems). Pooled DNA products were sequenced on the Illumina MiSeq Platform using 251 bp paired-end sequencing chemistry at the Microbial Community Sequencing Lab (University of Colorado Boulder).

QIIME2 (release 2021.2) was utilized to process resulting reads.[79] First, ITS reverse reads were discarded owing to low quality. After demultiplexing, DADA2 was utilized by QIIME2 on remaining reads to merge (pair-end read joining), quality filter (including denoising), check for chimeras, and bin to create amplicon sequence variants (ASVs).[80] As part of the denoising step, 16S forward reads were trimmed to 245 bp and reverse reads to 225 bp. For ITS data, forward reads were trimmed to 230 bp. Bacterial and archaeal (16S) ASVs were then assigned taxonomy using scikit-learn pretrained SILVA classifiers (version 138)[81−83] while fungal (ITS) ASVs were assigned taxonomy using self-trained UNITE database classifiers.[84,85] Resulting 16S rRNA gene read counts ranged from 586 to 26,221, and ITS amplicon sequencing read counts ranged from 901 to 23,527. Samples with low read counts (<1000) were included because rarefaction curves (produced using the function "rarecurve" in the vegan package in R) showed that we reached representative diversity in all samples (Figure S5). Finally, fungal ASVs were assigned to ecological guilds through FUNGuild if provided a single guild assignment with "highly probable" or "probable" confidence, per creator recommendations.[12,86] Resulting reads were deposited and are available at NCBI within BioProject PRJNA682830, and details are available in Supporting File 1.

Microbial Community Statistics. To assess the impacts of high severity burning of pyrocosms on the soil microbiome, statistical analyses were performed using R version 4.1.2 with significance accepted at $p < 0.05$.[87] Differences in species richness (alpha diversity) between the burned and unburned pyrocosms across the time series (Days 0 through 28) were tested using pairwise Wilcoxon signed-rank tests with a Bonferroni p-value adjustment for multiple tests using the function "stat_compare_means" in the package ggpubr[88] and the function "pairwise.wilcox.test" in the stats package.[87] Differences in bacterial/archaeal and fungal community composition were similarly assessed using nonparametric permutational multivariate analysis of variance (PERMANOVA)[89] using Bray−Curtis dissimilarity matrices and the "adonis2" function in the vegan package,[90] and these differences were subsequently visualized using Non-Metric Multidimensional Scaling (NMDS). Soil chemistry variables (carbon, nitrogen, and pH) and FUNGuild assignments were correlated with the resulting ordination space in the NMDSs using the "envfit" function in the vegan package with a Bonferroni p-value correction for multiple tests. Differences in beta dispersion between the burned and unburned microbial communities were assessed using the function "betadisper" in the vegan package and "anova" in the stats package. Next, coupled linear discriminant analysis effect size (LEfSe) and linear discriminant analysis (LDA) analyses were utilized to find taxa at the phyla, genera (bacterial/archaeal), and species (fungal) levels discriminant for either the burned or unburned pyrocosm conditions using the MicrobiomeAnalyst 2.0 server.[91] All visualizations were produced with the ggplot2 package,[92] except for combined LEfSe/LDA visualizations which came from MicrobiomeAnalyst 2.0[91] and formatted in Adobe Illustrator 2023 (v27.2). All statistical codes are available at https://github.com/julieafowler/Pyrocosm_Study_1Month.

Terminology. The organic matter collected from the burned soils is referred to as "SOM from burned soils." We cannot conclude with certainty that all the remaining organic matter in the burned soil was thermochemically altered by the fire nor are we using techniques that specifically target PyOM molecules such as polyaromatic hydrocarbons through the benzene polycarboxylic acids (BPCA) method[93,94] or levoglucosan biomarkers.[30,31] Therefore, it would be inaccurate to refer to all the organic matter collected from burned soils as PyOM. Consequently, we employ more conservative terminology ("SOM from burned soils") to describe the organic matter collected from burned soils which likely includes a mixture of PyOM, remaining SOM that was unaltered by fire, and molecules formed from the lysis and breakdown of microbes

https://doi.org/10.1021/acs.est.3c09797
Environ. Sci. Technol. 2024, 58, 4167−4180

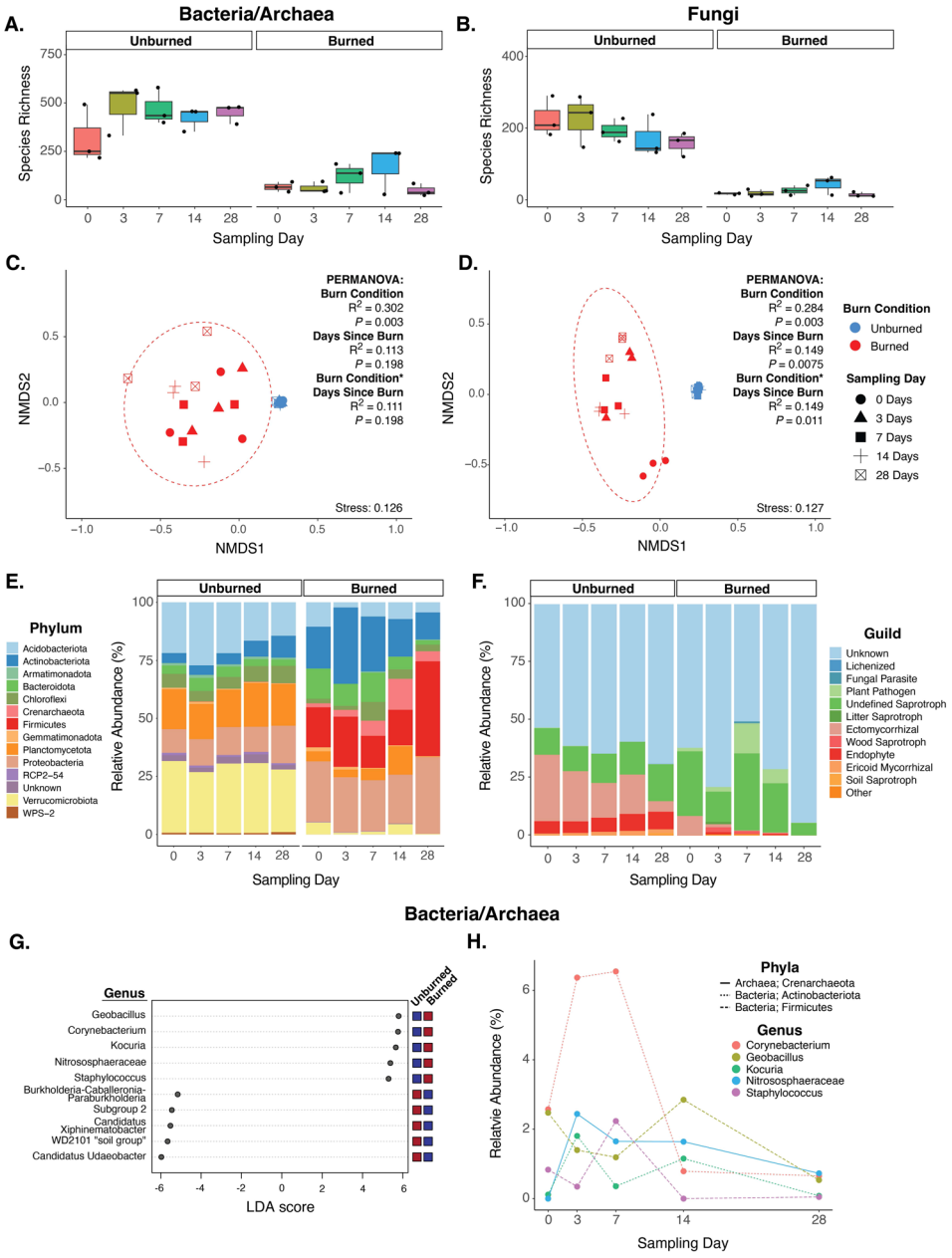

Figure 1. (A and B) Bacterial/archaeal (16S; A) and fungal (ITS; B) species richness box plots for burned and unburned pyrocosms. (C and D) Nonmetric multidimensional scaling (NMDS) ordination plots showing Bray−Curtis ASV microbial community composition dissimilarities for bacteria/archaea (16S; C) and fungi (ITS; D) including NMDS stress metrics and PERMANOVA test results. (E) Bar plot showing bacterial/archaeal phyla relative abundances between the unburned and burned pyrocosms averaged across replicates. (F) Bar chart showing the average relative abundances of samples within a given combination of burn condition and sampling day for fungal functional guilds as reported by FUNGuild (Nguyen et al., 2016).[86] The "other" category contains dung saprotroph, animal pathogen, orchid mycorrhizal, and lichen parasite guilds. (G) Dot plot showing the top ten results of Kruskal−Wallis rank sum tests followed by LDA analyses for biomarker discovery at the bacterial/archaeal genus level (16S). (H) Scatter plot of the average relative abundances of samples from burned pyrocosms of the top five genera from the combined LEfSe/LDA analysis on bacterial/archaeal genera in plot G.

and plant material. We operationally use the term "biodegradable" to describe SOM that can be metabolized by microbes across the time frame of this study, meaning that the SOM can be both physically accessed by microbes[42] and thermodynamically oxidized.[10]

Furthermore, we operationally use the term "metabolite" to refer to low-molecular weight, biodegradable molecules detected via nontargeted or targeted GC-MS analysis using authentic standards or curated spectral databases including saccharides, amino acids, and organic acids. The assemblage of these metabolites is referred to as the "metabolome." Our terminology is based on a methods paper published by Swenson et al. in which GC-MS is used to evaluate soil metabolomics.[53] Here, low molecular weight soil molecules such as carbohydrates, alcohols, sterols, and amino acids were referred to as metabolites and were detected with GC-MS.[53]

RESULTS AND DISCUSSION

Microbial Community Assemblage in Burned Soils is Altered and Contains Heterotrophic Microbes. Microbial

https://doi.org/10.1021/acs.est.3c09797
Environ. Sci. Technol. 2024, 58, 4167−4180

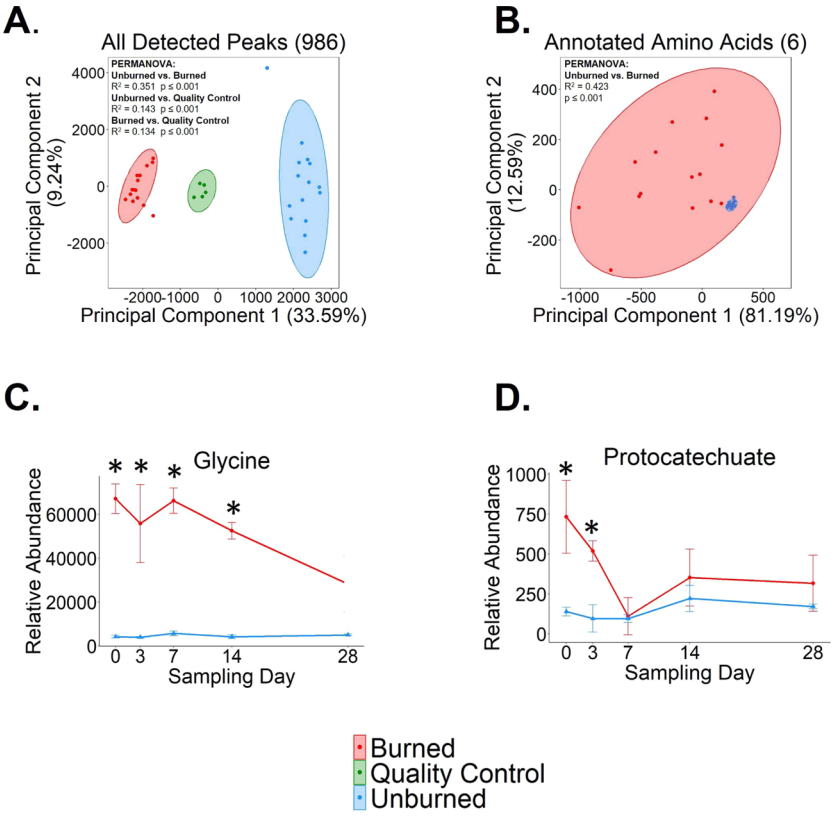

Figure 2. (A and B) Principal component analysis (PCA) score plots of a nontargeted GC-MS data set of water extracts from all 15 burned soil samples (three replicates for five sampling time points), all 15 unburned soil samples (three replicates for five sampling time points), and five quality control samples (prepared by mixing all the burned and unburned soil extracts and running five replicates of that mixture on the GC-MS instrument). The peak areas of detected peaks in the samples were normalized with total ion current normalization, scaled with Pareto scaling, and then used as the input data for the PCA scores plots. These normalized, scaled peak areas are indicative of metabolite relative abundance. (A) PCA score plot of peak areas for all 986 detected peaks. (B) PCA score plot of peak areas for six annotated amino acid peaks. PERMANOVA analysis was conducted to determine if the burned, unburned, and quality control groups were significantly different from each other for plots A and B. See Section 3 in the Supporting Information for details on PERMANOVA analysis. (C and D) Normalized abundances of annotated glycine peaks (C) and annotated protocatechuate peaks (D). Asterisk indicates a statistically significant difference between burned and unburned values within a given sampling day (t test, $p < 0.05$) ($n = 3$, error = standard deviation).

amplicon (16S/ITS) sequencing was utilized to assess postfire changes in microbial richness and community composition. Fire impacted the soil microbiome species richness (Figure 1A,B) and community composition (Figure 1C,D) while selecting for specific bacterial, archaeal, and fungal taxa and fungal guilds with potentially important roles in the postfire ecosystem. The immediate and persistent decrease in microbial richness in burned soils, in addition to the associated loss of ectomycorrhizal symbionts (Figure 1F), mirrors trends observed in prior high severity wildfire studies.[12,13,17,62,95] However, pairwise Wilcoxon signed-rank tests revealed no statistically significant differences in richness between burned and unburned samples at any given day postburn likely due to the low sampling size ($n = 3$) (Figure 1A,B). Nevertheless, multivariate analyses (nonmetric multidimensional scaling [NMDS] plots) revealed that burning led to distinct microbial communities and increased stochasticity compared to unburned conditions in both bacterial/archaeal and fungal soil communities (beta dispersion: $p = 2.317 \times 10^{-11}$ and $p = 2.2 \times 10^{-16}$, respectively) (Figures 1C,D and S6).

Heterotrophic microbes were detected in the burned soil samples with the phyla *Actinobacteria*, *Firmicutes*, and *Protobacteria* notably being enriched postfire (Figures 1E and S7A). These phyla contain heterotrophic species that could likely metabolize SOM in burned soils.[12,17,96] Other bacterial genera known to possess putative beneficial traits for the postfire ecosystem such as *Geobacillus* (spore formation)[97] and *Kocuria* (distribution via dust or smoke)[98] were also identified as discriminant taxa for burned soils (Figure 1G).

Burned Soils had Higher Concentrations of Water Extractable Organic Carbon. Water extractable organic carbon (WEOC) concentrations were measured to quantify carbon availability for microbial metabolism (Figure S8 and Table S4). The burned soil had statistically greater WEOC concentrations (t test, $p < 0.05$) across all sampling dates except for Day 28 despite there being no significant differences between the total carbon values of the burned and unburned soil for any sampling day (t test, $p < 0.05$) (Table S5). The WEOC results align with laboratory-based studies reporting increased WEOC in soils that were heated to approximately 250 °C.[19,20,99,100] The elevated WEOC content could be due to soil aggregate disruption, release of soluble organic compounds from cell lysis, and SOM oxidation during combustion.[12,57,100] WEOC is considered one of the most accessible fractions of carbon because WEOC can be transported through soil pores in water, bringing carbon that may not have been accessible otherwise to microbes.[70] Therefore, there is simply more WEOC in the burned soil

https://doi.org/10.1021/acs.est.3c09797
Environ. Sci. Technol. 2024, 58, 4167−4180

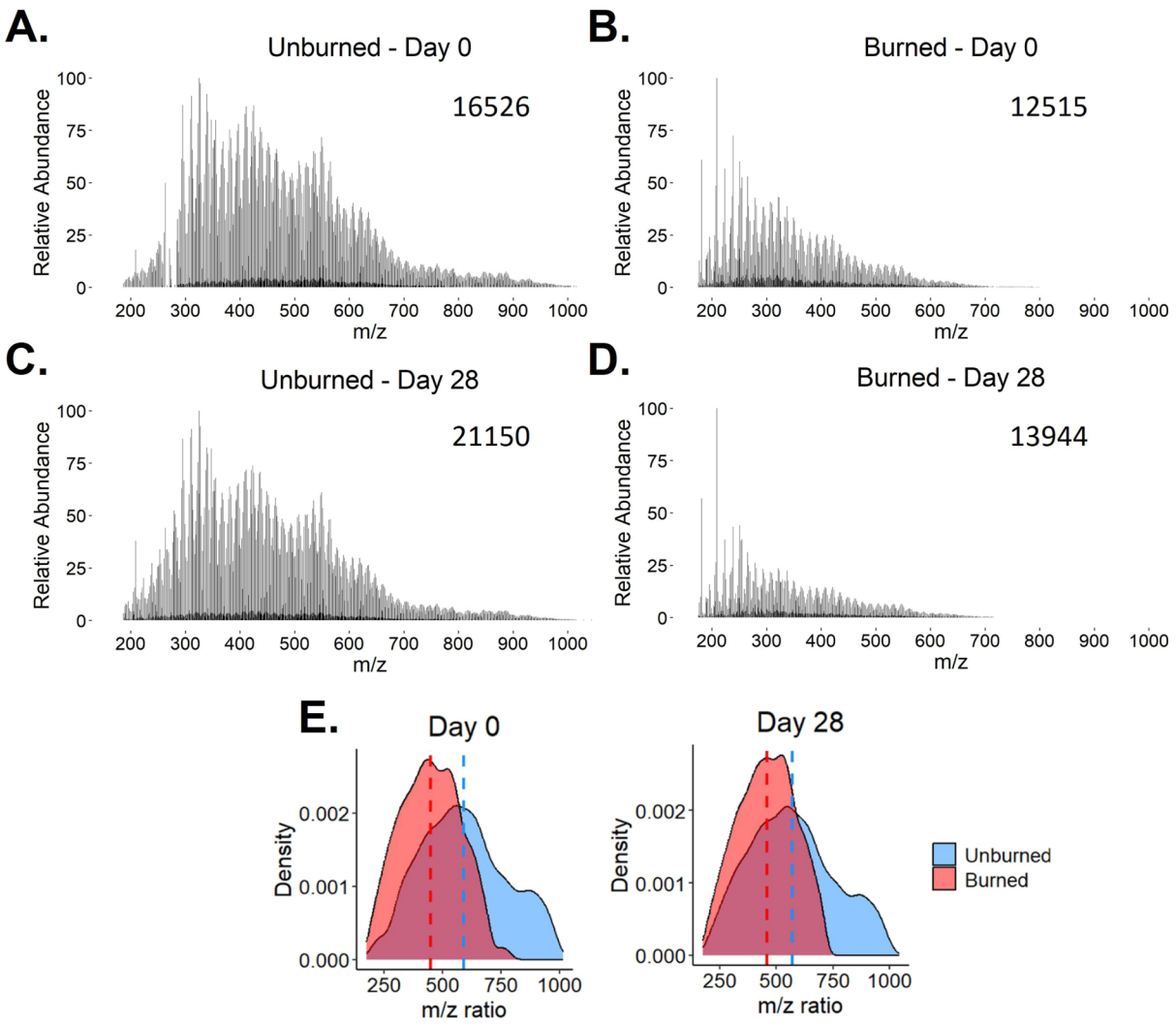

Figure 3. (A–D) FT ICR-MS mass spectra of peaks that were assigned molecular formulas from negative-mode electrospray ionization samples. The number in the upper-right corner of each spectrum is the total number of peaks that were assigned molecular formulas (including isotopes). (E) These m/z ratios were compiled into density plots. The y-axis indicates the relative probability of an ion featuring a given m/z ratio. The greater the density value for a given m/z ratio, the more ions that feature that m/z ratio. Dashed lines are mean values.

that heterotrophic microbes may metabolize. However, WEOC measurements do not assess molecular SOM composition which influences biodegradability.[10] Thus, two complementary mass spectrometry techniques were used to evaluate SOM composition.

Metabolites are Present in Burned Soils that may Support Microbial Activity. Normalized, scaled peak areas detected in nontargeted GC-MS analysis were plotted in principal component analysis (PCA) score plots to compare the metabolomic profiles of unburned and burned soils (Figure 2). A comparison of all detected peaks revealed statistically significant separate clustering of burned and unburned samples (Figure 2A) (PERMANOVA, $p \leq 0.001$), indicating that fire considerably altered the soil metabolite content. To explain differences in the burned and unburned metabolome, specific metabolite ontologies were examined.

Six amino acids were annotated in the samples via nontargeted analysis, and amino acid profiles were significantly different between burned and unburned samples (Figure 2B) (PERMANOVA, $p \leq 0.001$), likely contributing to the differences observed in the overall metabolome (Figure 2A). The unburned samples clustered closely among themselves in contrast to the more dispersed burned samples (Figure 2B). This suggests that fire considerably alters the soil amino acid abundances and/or amino acids abundances in burned soils are more susceptible to short-term (≤28 days) postfire changes.

The abundances of the annotated amino acids were either statistically similar between the burned and unburned samples or higher in the burned samples (Figures 2C and S9). Specifically, glycine was ∼16 times more abundant in the burned soil than the unburned soil for Day 0, potentially linked to the bacterial synthesis of glycine betaine which is a known thermoprotectant.[101,102] The higher amino acid abundances in burned soils may be due to protein denaturation or heat-induced microbial lysis which releases intracellular amino acids into the soil,[12] contributing to the "necromass zone" (an area of burned soil where remnants of dead microbes serve as biodegradable sources of carbon and nitrogen)[57] which may fuel postfire microbial metabolism.[56,103]

Microbes that could consume amino acids were detected in burned soil. *Crenarchaeota*, a thermophilic archaeal phyla, increased in relative abundance from less than 0.07% across the unburned soils to between 1.7% and 13.3% in the burned soils (Figure 1E).[104] One genera within this phyla, *Nitrososphaer-*

https://doi.org/10.1021/acs.est.3c09797
Environ. Sci. Technol. 2024, 58, 4167−4180

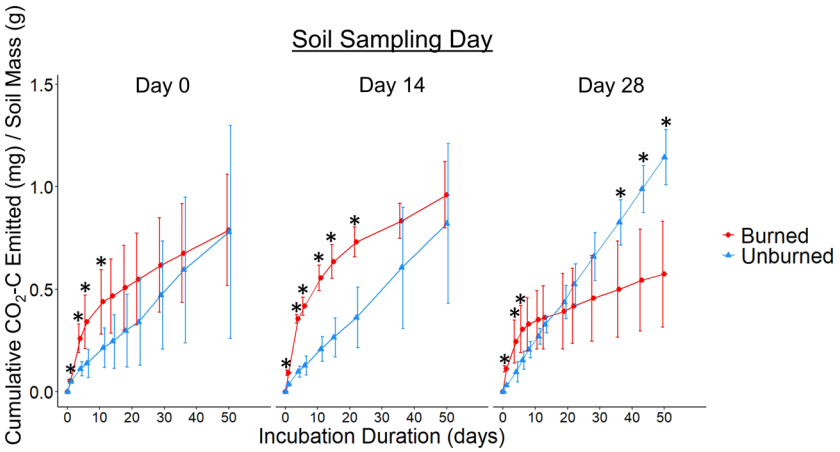

Figure 4. Cumulative CO_2−C emissions normalized to soil mass from burned and unburned soil incubations. Asterisk indicates a statistically significant difference (t test, $p < 0.05$) between burned and unburned values within a given incubation day ($n = 5$, error = standard deviation). Error bars were jittered to avoid overlap.

aceae, was identified as discriminant for burned samples using combined LEfSe/LDA analysis (Figures 1G,H). *Nitrososphaeraceae* are chemolithoautotrophic ammonia oxidizing archaea (AOA) and were potentially enriched by the elevated soil ammonium concentrations in the burned soil (Figure S10 and Table S6).[105−107] Additionally, *Nitrososphaeraceae* have been shown to uptake amino acids[108] and may have the potential for heterotrophic carbon utilization.[108−110] Therefore, AOA could utilize the enriched amino acids in the burned soil to fuel microbial metabolism.

Organic acids associated with citric acid cycle and saccharides were also annotated via nontargeted analysis in burned soil. Lactic acid, which is oxidized to pyruvic acid to enter the citric acid cycle, was statistically more abundant in burned soil for three sampling time points (t test, $p < 0.05$) (Figure S11A). Additionally, fumaric acid, succinic acid, and citric acid were all annotated in the burned and unburned soil samples (Figure S11). The annotated saccharide profiles of the burned and unburned soil samples were significantly different (Figure S12) (PERMANOVA, $p \leq 0.001$) with burned samples clustering tightly in contrast to highly dispersed unburned samples. Despite these differences in overall saccharide pool composition, there were no consistent patterns of saccharide enrichment in burned soils (Figures S13, see in Section 3 of the Supporting Information for how saccharides were annotated). Similarly to amino acids, organic acids and saccharides in burned soils were likely derived from heat-induced microbial lysis. The presence of organic acids and saccharides in burned soil further suggests that postfire soils contain biodegradable metabolites that could fuel microbial metabolism.

Detection of Catechol, Protocatechuate, and Citric Acid Cycle Metabolites Supports Aromatic Degradation Pathways. Catechol and protocatechuate were also detected in the burned and unburned soil via targeted metabolomics. Catechol abundances were not statistically different between burned and unburned soil whereas protocatechuate abundances were statistically greater in the burned soil for Day 0 and Day 3 (Figures 2D and S14). The targeted detection of catechol and protocatechuate supports proposed pathways of aromatic SOM degradation in burned soil in which catechol and protocatechuate are key intermediates.[12,39] Furthermore, the annotation of citric acid cycle intermediates further supports these pathways in which succinyl-CoA and acetyl-CoA (which feed into the citric acid cycle) are end products of aromatic degradation (Figure S11). These results support the second hypothesis of this study: while proposed intermediates in aromatic degradation pathways—namely, catechol, protocatechuate, and citric acid cycle metabolites—are detectable in both burned and unburned soils, the enrichment of specific metabolites (e.g., protocatechuate and lactic acid) in burned samples suggests that aromatic SOM may be degraded one-month after fire. Overall, we recommend that burned soil metabolomics be explored in both mesocosm and field studies to further elucidate the biogeochemical pathways governing postfire microbial and vegetative recovery.[111,112]

SOM from Burned Soils was Enriched in Nitrogen-Containing Compounds and Featured Lower Molecular Weights. FT-ICR MS analysis assigned thousands of molecular formulas with masses ranging from 175 to 1043 Da (Tables S2 and S3). The molecular formulas assigned in burned soil featured lower m/z ratios compared to unburned soil (Figures 3 and S15), potentially caused by the depolymerization of lignin-like, protein, and complex carbohydrate molecules.[31] This depolymerized organic matter may be more biodegradable because lower molecular-weight compounds are more easily accessible in the soluble pool, transported through cellular membranes, and subjected to microbial metabolism.[113]

There were also 20.1% to 43.1% more nitrogen-containing molecular formulas in burned soil compared to unburned soil (Figure S16), mirroring the increased water extractable total nitrogen values of burned soil (Figure S8, Table S7). Nitrogen enrichment in assigned molecular formulas was also observed in previous laboratory studies and may be due to the Maillard reaction pathway.[18,19,24] Nitrogen is often a limiting nutrient in soil systems;[114] thus, SOM enriched in nitrogen could serve as a nitrogen source for microbes in postfire environments, especially considering that the nitrogen-containing molecules in burned soils likely contain amino sugars and peptides according to van Krevelen analysis (Figures S17 and S18).[115]

Microbial Respiration is Stimulated in the Immediate Aftermath of Burning. Cumulative CO_2 emissions from Day 0, Day 14, and Day 28 soil were measured during 50-day incubations to determine if the burned soil microbiome was metabolically active and could mineralize SOM (Figure 4 and

https://doi.org/10.1021/acs.est.3c09797
Environ. Sci. Technol. 2024, 58, 4167−4180

Table S8). Day 0, Day 14, and Day 28 burned soil released significantly more CO_2 than the corresponding unburned soil for the first 12, 22, and 6 days of the incubations, respectively. Approximately 3.3 ± 1.1% and 3.7 ± 0.7% of the total soil carbon were released as CO_2−C from the burned and unburned soils, respectively, during the 50-day incubations. Overall, more CO_2 was initially released from the burned soil compared to the unburned soil, suggesting that heterotrophic microbes were consuming SOM in a complex burned soil environment. The CO_2−C emissions were also normalized to total soil carbon values (Figure S19 and Table S9) and featured the same differences between unburned and burned samples. When normalized to WEOC values, the ratio of CO_2−C to WEOC was generally greater in the unburned soil (Figure S20, Table S10). Additionally, the rates of CO_2−C emissions were initially greater in the burned soil (Figure S21 and Table S11).

CO_2 emissions were likely due to both physical and biotic factors. When water was added to the soil during incubation preparation, CO_2 in the soil pore spaces may have been physically displaced into the jar headspace; however, this process was likely restricted to the first few hours of incubation as evidenced by Marañón-Jiménez et al. who measured CO_2 respiration from burned soils in the Sierra Nevada Natural and National Parks.[116] After comparing decay rates of CO_2 flux after water was added to burned soil, they concluded that approximately 64% of soil CO_2 emissions during the first 2 h could be attributed to the release of CO_2 trapped in soil pores with the rest likely related to biological processes.[116] Thus, we anticipate that the physical displacement of CO_2 in our study was most likely restricted to the first few hours of incubation whereas the remaining CO_2 emissions were due to microbial respiration which can persist over weeks. For example, the biological mineralization of PyOM has been observed over the course of 57, 14, and 35 days in laboratory studies which are comparable time periods to the incubations conducted here.[23,39,117] Overall, the elevated WEOC content, enrichment of amino acids and organic acids, presence of saccharides, and detection of heterotrophic microbes in burned soil suggest that microbial mineralization of SOM contributed to the CO_2 emissions observed in these incubations.

Soil aggregate disruption may have contributed to the elevated CO_2 emissions in the burned soil. Soil aggregate stability can decrease after high intensity fires due to microbial biomass loss, SOM combustion, and dehydroxylation of clay minerals.[118−121] This aggregate disruption could make SOM more accessible by exposing physically protected SOM to microbial biodegradation, contributing to mineralization and CO_2 soil emissions.[100,122]

Considering that only ∼3.3% of total carbon in burned soil was released as CO_2 during the 50-day incubations, the readily biodegradable SOM pool in burned soil likely represents a relatively small fraction of the total SOM content.[117] Nevertheless, the soil CO_2 emission results support our first hypothesis that immediately after fire (i.e., the first 28 days), SOM in burned soil can be mineralized by microbes in a complex, burned soil environment.

Overall, this study demonstrated that readily biodegradable SOM is present and accessible by microbes within mineral soils immediately after a simulated high intensity burn. Burned soil had more WEOC which likely fueled CO_2 emissions despite lower microbial richness. Concurrently, the detection of putative, heterotrophic microbes in the burned soil represents a mechanism via which SOM in burned soil is mineralized.[40,41] The identification of enriched metabolites (i.e., glycine and other amino acids, some saccharides, protocatechuate) in burned soil offers insight into the SOM pools that may be available for microbial metabolism postfire. Finally, this study demonstrated that pyrocosms can be used to evaluate postfire soil dynamics beyond analyzing shifts in fungal community composition as pioneered by Bruns et al.[57]

Environmental Implications. The metabolism of SOM in complex burned soils observed in this study supports the laboratory-based studies that reported rapid biodegradation of PyOM,[38−41,117] and our findings provide further evidence for the degradation pathways of aromatic compounds in burned soils.[12,39] Our characterization of organic acids, amino acids, and saccharides advances our collective understanding of what substrates are available for microbial metabolism in burned soils that can fuel postfire soil recovery. The loss of ectomycorrhizal fungi after burning (Figure 1F)—which may have been impacted by soil disturbance and separation from plant hosts during soil sampling and pyrocosm assembly—and decreases in fungal diversity after burning (Figure 1B) have implications for nutrient transport through fungal networks and may constrain the recovery of ectomycorrhizal-obligate species such as lodgepole pine. However, the detection of heterotrophic microbes, presence of biodegradable SOM, and observed postfire metabolism highlight the resilience of soil systems in response to high severity burns which are projected to increase due to climate change.[6]

Wildfires are well-known to be fatal to many soil microbial taxa and to generate persistent forms of SOM.[12,13,37,123] However, our study highlights that both biodegradable forms of SOM and heterotrophic microbes are present after extreme soil heating. The variety of detected SOM in this study suggests that SOM in burned soil is comprised of a diverse array of chemical compounds (e.g., PyOM, SOM that was not thermochemically altered, and intracellular metabolites released from cell lysis) that feature varying degrees of biodegradability. Thus, severely burned environments are not dominated solely by PyOM and are not sterile. Rather, our experimental burns demonstrated that the surviving soil microbiome was active and able to metabolize the heterogeneous SOM in the burned soil.

■ ASSOCIATED CONTENT

Supporting Information

: The Supporting Information is available free of charge at https://pubs.acs.org/doi/10.1021/acs.est.3c09797.

Table demonstrating what analytical techniques were used on which soil samples, number of assigned molecular formulas and m/z ratios from FT-ICR MS data, soil CO_2 emission results, total carbon results, total nitrogen results, pH results, water-extractable organic carbon and water-extractable total nitrogen results, ammonium results, schematic of pyrocosm, pyrocosm photos, soil temperature of the burned pyrocosms, schematic for soil sampling schedule, rarefaction curves, microbial nonmetric multidimensional scaling ordination plots, microbial relative abundance data, normalized relative abundances of annotated metabolites, PCA scores plot of saccharide data, FT-ICR MS m/z density plot and nitrogen-containing formulas bar plots, van Krevelen diagrams, CO_2 respiration rate results and

https://doi.org/10.1021/acs.est.3c09797
Environ. Sci. Technol. 2024, 58, 4167−4180

cumulative CO_2 emissions normalized to total carbon and WEOC, rationale for the use of pyrocosms, GC-MS experimental procedure, and FT-ICR MS experimental procedure (PDF)

Details related to microbial read counts that are available at NCBI within BioProject PRJNA682830 (XLSX)

AUTHOR INFORMATION

Corresponding Author

Thomas Borch − *Department of Chemistry and Department of Soil and Crop Sciences, Colorado State University, Fort Collins, Colorado 80521, United States;* orcid.org/0000-0002-4251-1613; Phone: +1 (970) 491-6235; Email: thomas.borch@colostate.edu

Authors

Jacob P. VanderRoest − *Department of Chemistry, Colorado State University, Fort Collins, Colorado 80521, United States*

Julie A. Fowler − *Department of Soil and Crop Sciences, Colorado State University, Fort Collins, Colorado 80521, United States*

Charles C. Rhoades − *Rocky Mountain Research Station, U.S. Forest Service, Fort Collins, Colorado 80526, United States*

Holly K. Roth − *Department of Soil and Crop Sciences, Colorado State University, Fort Collins, Colorado 80521, United States;* orcid.org/0000-0003-2733-517X

Corey D. Broeckling − *Bioanalysis and Omics Center, Analytical Resources Core, Colorado State University, Fort Collins 80521, United States;* orcid.org/0000-0002-6158-827X

Timothy S. Fegel − *Rocky Mountain Research Station, U.S. Forest Service, Fort Collins, Colorado 80526, United States*

Amy M. McKenna − *Department of Soil and Crop Sciences, Colorado State University, Fort Collins, Colorado 80521, United States; National High Magnetic Field Laboratory, Florida State University, Tallahassee, Florida 32310, United States*

Emily K. Bechtold − *Department of Soil and Crop Sciences, Colorado State University, Fort Collins, Colorado 80521, United States*

Claudia M. Boot − *Department of Chemistry, Colorado State University, Fort Collins, Colorado 80521, United States*

Michael J. Wilkins − *Department of Soil and Crop Sciences, Colorado State University, Fort Collins, Colorado 80521, United States*

Complete contact information is available at: https://pubs.acs.org/10.1021/acs.est.3c09797

Author Contributions

The manuscript was written through contributions of all authors. All authors have given approval to the final version of the manuscript.

Notes

The authors declare no competing financial interest.

ACKNOWLEDGMENTS

This research was funded by M.J.W. and T.B. from the National Science Foundation under grant number 2114868 and the United States Department of Agriculture (USDA) National Institute of Food and Agriculture through AFRI grant number 2021-67019-34608. The Table of Contents artwork was created with BioRender.com. We thank Troy Bauder, Karl Whitman, and the Poudre Fire Authority for providing a safe location for the pyrocosm burns. We thank Daniel Reuss and the EcoCore facility at Colorado State University for assisting with soil CO_2 measurements and total soil C and N measurements. GC-MS was performed at the CSU ARC-BIO facility (RRID: SCR_021758). Thanks to Dr. Prithwiraj De for helping with GC-MS derivatization and sample preparation. Thanks to Dr. Robert Young for providing code for the FT-ICR MS data analysis. Thanks to researchers at the Rocky Mountain Research Station biogeochemistry lab, owned by the USDA Forest Service, for conducting dissolved organic carbon, dissolved total nitrogen, and ammonium measurements. Thanks to researchers at the National High Magnetic Field Laboratory ICR User Facility which is supported by the National Science Foundation Division of Chemistry and Division of Material Research through DMR-1644779 and DMR-2128556. Data for this research were provided by the Niwot Ridge LTER program (NWT VII: NSF DEB-1637686, NWT VIII: NSF DEB-2224439). Use of firm, trade, or product names is for descriptive purposes only and does not imply indorsement by the U.S. government.

REFERENCES

(1) NIFC. *National Large Incident Year-to-Date Report*, 2020.

(2) Hoover, K.; Hanson, L. A. *Wildfire Statistics*; Congressional Research Service, 2021; pp 2.

(3) Nolan, R. H.; Boer, M. M.; Collins, L.; Resco De Dios, V.; Clarke, H.; Jenkins, M.; Kenny, B.; Bradstock, R. A. Causes and consequences of eastern Australia's 2019−20 season of mega-fires. *Global Change Biol.* **2020**, *26* (3), 1039−1041.

(4) Pausas, J. G.; Keeley, J. E. Wildfires as an ecosystem service. *Front. Ecol. Environ.* **2019**, *17* (5), 289−295.

(5) Keeley, J. E. Fire intensity, fire severity and burn severity: A brief review and suggested usage. *Int. J. Wildland Fire* **2009**, *18* (1), 116.

(6) Jones, M. W.; Abatzoglou, J. T.; Veraverbeke, S.; Andela, N.; Lasslop, G.; Forkel, M.; Smith, A. J. P.; Burton, C.; Betts, R. A.; Van Der Werf, G. R.; Sitch, S.; Canadell, J. G.; Santín, C.; Kolden, C.; Doerr, S. H.; Le Quéré, C. Global and Regional Trends and Drivers of Fire Under Climate Change. *Rev. Geophys.* **2022**, *60* (3), 1.

(7) Brucker, C. P.; Livneh, B.; Minear, J. T.; Rosario-Ortiz, F. L. A review of simulation experiment techniques used to analyze wildfire effects on water quality and supply. *Environ. Sci.* **2022**, *24* (8), 1110−1132.

(8) Higuera, P. E.; Cook, M. C.; Balch, J. K.; Stavros, E. N.; Mahood, A. L.; St. Denis, L. A. Shifting social-ecological fire regimes explain increasing structure loss from Western wildfires. *PNAS Nexus* **2023**, *2*, pgad005.

(9) González-Pérez, J. A.; González-Vila, F. J.; Almendros, G.; Knicker, H. The effect of fire on soil organic matter—a review. *Environ. Int.* **2004**, *30* (6), 855−870.

(10) Larowe, D. E.; Van Cappellen, P. Degradation of natural organic matter: A thermodynamic analysis. *Geochim. Cosmochim. Acta* **2011**, *75* (8), 2030−2042.

(11) Pressler, Y.; Moore, J. C.; Cotrufo, M. F. Belowground community responses to fire: meta-analysis reveals contrasting responses of soil microorganisms and mesofauna. *Oikos* **2019**, *128* (3), 309−327.

(12) Nelson, A. R.; Narrowe, A. B.; Rhoades, C. C.; Fegel, T. S.; Daly, R. A.; Roth, H. K.; Chu, R. K.; Amundson, K. K.; Young, R. B.; Steindorff, A. S.; Mondo, S. J.; Grigoriev, I. V.; Salamov, A.; Borch, T.; Wilkins, M. J. Wildfire-dependent changes in soil microbiome diversity and function. *Nat. Microbiol.* **2022**, *7* (9), 1419−1430.

(13) Caiafa, M. V.; Nelson, A. R.; Borch, T.; Roth, H. K.; Fegel, T.; Rhoades, C. C.; Wilkins, M. J.; Glassman, S. I. Distinct fungal and bacterial responses to fire severity and soil depth across a ten-year wildfire chronosequence in bettle-killed lodgepole pine forests. *For. Ecol. Manage.* **2023**, *544*, 121160.

(14) Woolet, J.; Whitman, T. Pyrogenic organic matter effects on soil bacterial community composition. *Soil Biol. Biochem.* **2020**, *141*, 107678.
(15) Whitman, T.; Whitman, E.; Woolet, J.; Flannigan, M. D.; Thompson, D. K.; Parisien, M.-A. Soil bacterial and fungal response to wildfires in the Canadian boreal forest across a burn severity gradient. *Soil Biol. Biochem.* **2019**, *138*, 107571.
(16) Whitman, T.; Pepe-Ranney, C.; Enders, A.; Koechli, C.; Campbell, A.; Buckley, D. H.; Lehmann, J. Dynamics of microbial community composition and soil organic carbon mineralization in soil following addition of pyrogenic and fresh organic matter. *Isme J.* **2016**, *10* (12), 2918−2930.
(17) Enright, D. J.; Frangioso, K. M.; Isobe, K.; Rizzo, D. M.; Glassman, S. I. Mega-fire in redwood tanoak forest reduces bacterial and fungal richness and selects for pyrophilous taxa that are phylogenetically conserved. *Mol. Ecol.* **2022**, *31* (8), 2475−2493.
(18) Roth, H. K.; McKenna, A. M.; Simpson, M. J.; Chen, H.; Srikanthan, N.; Fegel, T.; Nelson, A. R.; Rhoades, C. C.; Wilkins, M. J.; Borch, T. Effects of burn severity on organic nitrogen and carbon chemsitry in high-elevation forest soils. *Soil Environ. Health* **2023**, *1*, 100023.
(19) Bahureksa, W.; Young, R. B.; McKenna, A. M.; Chen, H.; Thorn, K. A.; Rosario-Ortiz, F. L.; Borch, T. Nitrogen Enrichment during Soil Organic Matter Burning and Molecular Evidence of Maillard Reactions. *Environ. Sci. Technol.* **2022**, *56* (7), 4597−4609.
(20) Cawley, K. M.; Hohner, A. K.; Podgorski, D. C.; Cooper, W. T.; Korak, J. A.; Rosario-Ortiz, F. L. Molecular and Spectroscopic Characterization of Water Extractable Organic Matter from Thermally Altered Soils Reveal Insight into Disinfection Byproduct Precursors. *Environ. Sci. Technol.* **2017**, *51* (2), 771−779.
(21) Knicker, H. How does fire affect the nature and stability of soil organic nitrogen and carbon? A review. *Biogeochemistry* **2007**, *85* (1), 91−118.
(22) Bird, M. I.; Wynn, J. G.; Saiz, G.; Wurster, C. M.; McBeath, A. The Pyrogenic Carbon Cycle. *Annu. Rev. Earth Planet. Sci.* **2015**, *43* (1), 273−298.
(23) Zimmerman, A. R. Abiotic and Microbial Oxidation of Laboratory-Produced Black Carbon (Biochar). *Environ. Sci. Technol.* **2010**, *44* (4), 1295−1301.
(24) Roth, H. K.; Borch, T.; Young, R. B.; Bahureksa, W.; Blakney, G. T.; Nelson, A. R.; Wilkins, M. J.; McKenna, A. M. Enhanced Speciation of Pyrogenic Organic Matter from Wildfires Enabled by 21 T FT-ICR Mass Spectrometry. *Anal. Chem.* **2022**, *94* (6), 2973−2980.
(25) Zhang, Y.; Biswas, A. The Effects of Forest Fire on Soil Organic Matter and Nutrients in Boreal Forests of North America: A Review. In *Adaptive Soil Management: From Theory to Practices*; Springer: Singapore, 2017; pp 465476. DOI: .
(26) Torres-Rojas, D.; Hestrin, R.; Solomon, D.; Gillespie, A. W.; Dynes, J. J.; Regier, T. Z.; Lehmann, J. Nitrogen speciation and transformations in fire-derived organic matter. *Geochim. Cosmochim. Acta* **2020**, *276*, 170−185.
(27) Pellegrini, A. F. A.; Harden, J.; Georgiou, K.; Hemes, K. S.; Malhotra, A.; Nolan, C. J.; Jackson, R. B. Fire effects on the persistence of soil organic matter and long-term carbon storage. *Nat. Geosci.* **2021**, *15*, 5−13.
(28) Pellegrini, A. F. A.; Ahlström, A.; Hobbie, S. E.; Reich, P. B.; Nieradzik, L. P.; Staver, A. C.; Scharenbroch, B. C.; Jumpponen, A.; Anderegg, W. R. L.; Randerson, J. T.; Jackson, R. B. Fire frequency drives decadal changes in soil carbon and nitrogen and ecosystem productivity. *Nature* **2018**, *553* (7687), 194−198.
(29) Wagner, S.; Coppola, A. I.; Stubbins, A.; Dittmar, T.; Niggemann, J.; Drake, T. W.; Seidel, M.; Spencer, R. G. M.; Bao, H. Questions remain about the biolability of dissolved black carbon along the combustion continuum. *Nat. Commun.* **2021**, *12*, 1.
(30) Myers-Pigg, A. N.; Louchouarn, P.; Amon, R. M. W.; Prokushkin, A.; Pierce, K.; Rubtsov, A. Labile pyrogenic dissolved organic carbon in major Siberian Arctic rivers: Implications for wildfire-stream metabolic linkages. *Geophys. Res. Lett.* **2015**, *42* (2), 377−385.
(31) Norwood, M. J.; Louchouarn, P.; Kuo, L.-J.; Harvey, O. R. Characterization and biodegradation of water-soluble biomarkers and organic carbon extracted from low temperature chars. *Org. Geochem.* **2013**, *56*, 111−119.
(32) Hestrin, R.; Torres-Rojas, D.; Dynes, J. J.; Hook, J. M.; Regier, T. Z.; Gillespie, A. W.; Smernik, R. J.; Lehmann, J. Fire-derived organic matter retains ammonia through covalent bond formation. *Nat. Commun.* **2019**, *10*, 1.
(33) Lutfalla, S.; Abiven, S.; Barre, P.; Wiedemeier, D. B.; Christensen, B. T.; Houot, S.; Katterer, T.; Macdonald, A. J.; van Oort, F.; Chenu, C. Pyrogenic Carbon Lacks Long-Term Persistence in Temperate Arable Soils. *Front. Earth Sci.* **2017**, *5*, 96.
(34) Bowring, S. P. K.; Jones, M. W.; Ciais, P.; Guenet, B.; Abiven, S. Pyrogenic carbon decomposition critical to resolving fire's role in the Earth system. *Nat. Geosci.* **2022**, *15* (2), 135−142.
(35) Coppola, A. I.; Wagner, S.; Lennartz, S. T.; Seidel, M.; Ward, N. D.; Dittmar, T.; Santín, C.; Jones, M. W. The black carbon cycle and its role in the Earth system. *Nat. Rev. Earth Environ.* **2022**, *3* (8), 516−532.
(36) Santín, C.; Doerr, S. H.; Kane, E. S.; Masiello, C. A.; Ohlson, M.; De La Rosa, J. M.; Preston, C. M.; Dittmar, T. Towards a global assessment of pyrogenic carbon from vegetation fires. *Global Change Biol.* **2016**, *22* (1), 76−91.
(37) Liang, B.; Lehmann, J.; Solomon, D.; Sohi, S.; Thies, J. E.; Skjemstad, J. O.; Luizao, F. J.; Engelhard, M. H.; Neves, E. G.; Wirick, S. Stability of biomass-derived black carbon in soils. *Geochim. Cosmochim. Acta* **2008**, *72*, 6069−6078.
(38) De La Rosa, J. M.; Miller, A. Z.; Knicker, H. Soil-borne fungi challenge the concept of long-term biochemical recalcitrance of pyrochar. *Sci. Rep.* **2018**, *8*, 1.
(39) Fischer, M. S.; Stark, F. G.; Berry, T. D.; Zeba, N.; Whitman, T.; Traxler, M. F. Pyrolyzed Substrates Induce Aromatic Compound Metabolism in the Post-fire Fungus, Pyronema domesticum. *Front. Microbiol.* **2021**, *12*, 729289.
(40) Goranov, A. I.; Wozniak, A. S.; Bostick, K. W.; Zimmerman, A. R.; Mitra, S.; Hatcher, P. G. Microbial labilization and diversification of pyrogenic dissolved organic matter. *Biogeosciences* **2022**, *19* (5), 1491−1514.
(41) Bostick, K. W.; Zimmerman, A. R.; Goranov, A. I.; Mitra, S.; Hatcher, P. G.; Wozniak, A. S. Biolability of Fresh and Photodegraded Pyrogenic Dissolved Organic Matter From Laboratory-Prepared Chars. *J. Geophys. Res.: Biogeosci.* **2021**, *126* (5), 1−17.
(42) Schmidt, M. W. I.; Torn, M. S.; Abiven, S.; Dittmar, T.; Guggenberger, G.; Janssens, I. A.; Kleber, M.; Kögel-Knabner, I.; Lehmann, J.; Manning, D. A. C.; Nannipieri, P.; Rasse, D. P.; Weiner, S.; Trumbore, S. E. Persistence of soil organic matter as an ecosystem property. *Nature* **2011**, *478* (7367), 49−56.
(43) Yang, F.; Xu, Z.; Yu, L.; Gao, B.; Xu, X.; Zhao, L.; Cao, X. Kaolinite Enhances the Stability of the Dissolvable and Undissolvable Fractions of Biochar via Different Mechanisms. *Environ. Sci. Technol.* **2018**, *52* (15), 8321−8329.
(44) Yang, F.; Xu, Z.; Huang, Y.; Tsang, D. C. W.; Sik Ok, Y.; Zhao, L.; Qiu, H.; Xu, X.; Cao, X. Stabilization of dissolvable biochar by soil minerals: Release reduction and organo-mineral complexes formation. *J. Hazard. Mater.* **2021**, *412*, 125213.
(45) Wang, M.; Schoettner, M.; Xu, S.; Paetz, C.; Wilde, J.; Baldwin, I. T.; Groten, K. Catechol, a major component of smoke, influences primary root growth and root hair elongation through reactive oxygen species-mediated redox signaling. *New Phytol.* **2017**, *213* (4), 1755−1770.
(46) De La Rosa, J. M.; González-Pérez, J. A.; González-Vázquez, R.; Knicker, H.; López-Capel, E.; Manning, D. A. C.; González-Vila, F. J. Use of pyrolysis/GC−MS combined with thermal analysis to monitor C and N changes in soil organic matter from a Mediterranean fire affected forest. *CATENA* **2008**, *74* (3), 296−303.
(47) Jiménez-González, M. A.; De La Rosa, J. M.; Jiménez-Morillo, N. T.; Almendros, G.; González-Pérez, J. A.; Knicker, H. Post-fire

recovery of soil organic matter in a Cambisol from typical Mediterranean forest in Southwestern Spain. *Sci. Total Environ.* **2016**, *572*, 1414−1421.
(48) Faria, S. R.; De La Rosa, J. M.; Knicker, H.; González-Pérez, J. A.; Keizer, J. J. Molecular characterization of wildfire impacts on organic matter in eroded sediments and topsoil in Mediterranean eucalypt stands. *CATENA* **2015**, *135*, 29−37.
(49) Jiménez-Morillo, N. T.; de la Rosa, J. M.; Waggoner, D.; Almendros, G.; González-Vila, F. J.; González-Pérez, J. A. Fire effects in the molecular structure of soil organic matter fractions under Quercus suber cover. *CATENA* **2016**, *145*, 266−273.
(50) Jiménez-Morillo, N. T.; Almendros, G.; De la Rosa, J. M.; Jordán, A.; Zavala, L. M.; Granged, A. J. P.; González-Pérez, J. A. Effect of a wildfire and of post-fire restoration actions in the organic matter structure in soil fractions. *Sci. Total Environ.* **2020**, *728*, 138715.
(51) Chen, H.; Wang, J.-J.; Ku, P.-J.; Tsui, M. T.-K.; Abney, R. B.; Berhe, A. A.; Zhang, Q.; Burton, S. D.; Dahlgren, R. A.; Chow, A. T. Burn Intensity Drives the Alteration of Phenolic Lignin to (Poly) Aromatic Hydrocarbons as Revealed by Pyrolysis Gas Chromatography−Mass Spectrometry (Py-GC/MS). *Environ. Sci. Technol.* **2022**, *56* (17), 12678−12687.
(52) Seitz, V. A.; McGivern, B. B.; Daly, R. A.; Chaparro, J. M.; Borton, M. A.; Sheflin, A. M.; Kresovich, S.; Shields, L.; Schipanski, M. E.; Wrighton, K. C.; Prenni, J. E.; Alexandre, G. Variation in Root Exudate Composition Influences Soil Microbiome Membership and Function. *Appl. Environ. Microbiol.* **2022**, *88* (11), 1.
(53) Swenson, T. L.; Jenkins, S.; Bowen, B. P.; Northen, T. R. Untargeted soil metabolomics methods for analysis of extractable organic matter. *Soil Biol. Biochem.* **2015**, *80*, 189−198.
(54) Bahureksa, W.; Borch, T.; Young, R. B.; Weisbrod, C. R.; Blakney, G. T.; McKenna, A. M. Improved Dynamic Range, Resolving Power, and Sensitivity Achievable with FT-ICR Mass Spectrometry at 21 T Reveals the Hidden Complexity of Natural Organic Matter. *Anal. Chem.* **2022**, *94* (32), 11382−11389.
(55) Jiménez-Morillo, N. T.; González-Pérez, J. A.; Almendros, G.; De la Rosa, J. M.; Waggoner, D. C.; Jordan, A.; Zavala, L. M.; González-Vila, F. J.; Hatcher, P. G. Ultra-high resolution mass spectrometry of physical speciation patterns of organic matter in fire-affected soils. *J. Environ. Manage.* **2018**, *225*, 139−147.
(56) Zhang, Q.; Wang, Y.; Guan, P.; Zhang, P.; Mo, X.; Yin, G.; Qu, B.; Xu, S.; He, C.; Shi, Q.; Zhang, G.; Dittmar, T.; Wang, J. Temperature Thresholds of Pyrogenic Dissolved Organic Matter in Heating Experiments Simulating Forest Fires. *Environ. Sci. Technol.* **2023**, *57*, 17291−17301.
(57) Bruns, T. D.; Chung, J. A.; Carver, A. A.; Glassman, S. I.; Suen, G. A simple pyrocosm for studying soil microbial response to fire reveals a rapid, massive response by Pyronema species. *PLoS One* **2020**, *15*, 3.
(58) Long Draw Reservoir SNOTEL Site 1123 Database. United States Department of Agriculture Natural Resources Convservation Service National Water and Climate Center. https://wcc.sc.egov.usda.gov/nwcc/site?sitenum=1123. (accessed 2023−September−18).
(59) Roshan, A.; Biswas, A. Fire-induced geochemical changes in soil: Implication for the element cycling. *Sci. Total Environ.* **2023**, *868*, 161714.
(60) Colorado State University. CoAgMet Daily Summary Access Database. https://coagmet.colostate.edu/cgi-bin/dailysum_form.pl (accessed 2023−September−18).
(61) Novara, A.; Gristina, L.; Bodì, M. B.; Cerdá, A. The impact of fire on redistribution of soil organic matter on a mediterranean hillslope under maquia vegetation type. *Land Degrad. Dev.* **2011**, *22* (6), 530−536.
(62) Dove, N. C.; Taş, N.; Hart, S. C. Ecological and genomic responses of soil microbiomes to high-severity wildfire: Linking community assembly to functional potential. *Isme J.* **2022**, *16* (7), 1853−1863.
(63) Emmett, M. R.; White, F. M.; Hendrickson, C. L.; Shi, S. D. H.; Marshall, A. G. Application of micro-electrospray liquid chromatography techniques to FT-ICR MS to enable high-sensitivity biological analysis. *J. Am. Soc. Mass Spectrom.* **1998**, *9* (4), 333−340.
(64) Hendrickson, C. L.; Quinn, J. P.; Kaiser, N. K.; Smith, D. F.; Blakney, G. T.; Chen, T.; Marshall, A. G.; Weisbrod, C. R.; Beu, S. C. 21 Tesla Fourier Transform Ion Cyclotron Resonance Mass Spectrometer: A National Resource for Ultrahigh Resolution Mass Analysis. *J. Am. Soc. Mass Spectrom.* **2015**, *26* (9), 1626−1632.
(65) Smith, D. F.; Podgorski, D. C.; Rodgers, R. P.; Blakney, G. T.; Hendrickson, C. L. 21 Tesla FT-ICR Mass Spectrometer for Ultrahigh-Resolution Analysis of Complex Organic Mixtures. *Anal. Chem.* **2018**, *90* (3), 2041−2047.
(66) Xian, F.; Hendrickson, C. L.; Blakney, G. T.; Beu, S. C.; Marshall, A. G. Automated Broadband Phase Correction of Fourier Transform Ion Cyclotron Resonance Mass Spectra. *Anal. Chem.* **2010**, *82* (21), 8807−8812.
(67) Savory, J. J.; Kaiser, N. K.; McKenna, A. M.; Xian, F.; Blakney, G. T.; Rodgers, R. P.; Hendrickson, C. L.; Marshall, A. G. Parts-Per-Billion Fourier Transform Ion Cyclotron Resonance Mass Measurement Accuracy with a "Walking" Calibration Equation. *Anal. Chem.* **2011**, *83* (5), 1732−1736.
(68) Kendrick, E. A Mass Scale Based on CH_2 = 14.0000 for High Resolution Mass Spectrometry of Organic Compounds. *Anal. Chem.* **1963**, *35* (13), 2146−2154.
(69) Hughey, C. A.; Hendrickson, C. L.; Rodgers, R. P.; Marshall, A. G.; Qian, K. Kendrick Mass Defect Spectrum: A Compact Visual Analysis for Ultrahigh-Resolution Broadband Mass Spectra. *Anal. Chem.* **2001**, *73* (19), 4676−4681.
(70) Bahureksa, W.; Tfaily, M. M.; Boiteau, R. M.; Young, R. B.; Logan, M. N.; McKenna, A. M.; Borch, T. Soil Organic Matter Characterization by Fourier Transform Ion Cyclotron Resonance Mass Spectrometry (FTICR MS): A Critical Review of Sample Preparation, Analysis, and Data Interpretation. *Environ. Sci. Technol.* **2021**, *55* (14), 9637−9656.
(71) Corilo, Y. E. *PetroOrg. Software*; Florida State University, Omics LLC: Tallahassee, FL, 2014.
(72) Vetter, W. F. W.; McLafferty, F. T. Interpretation of Mass Spectra, 4 th ed.; University Science Books: Mill Valley, California, 1994; Vol. *23*, pp 379.
(73) Kind, T.; Fiehn, O. Seven Golden Rules for heuristic filtering of molecular formulas obtained by accurate mass spectrometry. *BMC Bioinf.* **2007**, *8* (1), 105.
(74) Cotrufo, M. F.; Soong, J. L.; Horton, A. J.; Campbell, E. E; Haddix, M. L.; Wall, D. H.; Parton, W. J. Formation of soil organic matter via biochemical and physical pathways of litter mass loss. *Nat. Geosci.* **2015**, *8* (10), 776−779.
(75) Parada, A. E.; Needham, D. M.; Fuhrman, J. A. Every base matters: assessing small subunit rRNA primers for marine microbiomes with mock communities, time series and global field samples. *Environ. Microbiol.* **2016**, *18* (5), 1403−1414.
(76) Apprill, A.; McNally, S.; Parsons, R.; Weber, L. Minor revision to V4 region SSU rRNA 806R gene primer greatly increases detection of SAR11 bacterioplankton. *Aquat. Microb. Ecol.* **2015**, *75* (2), 129−137.
(77) White, T. J.; Bruns, T.; Lee, S.; Taylor, J. Amplification and direct sequencing of fungal ribosomal RNA genes for phylogenetics. *PCR protocols: A guide to methods and applications*; Academic Press: New York, 1990; pp. 315322.
(78) Thompson, L. R.; Sanders, J. G.; McDonald, D.; Amir, A.; Ladau, J.; Locey, K. J.; Prill, R. J.; Tripathi, A.; Gibbons, S. M.; Ackermann, G.; Navas-Molina, J. A.; Janssen, S.; Kopylova, E.; Vázquez-Baeza, Y.; González, A.; Morton, J. T.; Mirarab, S.; Zech Xu, Z.; Jiang, L.; Haroon, M. F.; Kanbar, J.; Zhu, Q.; Jin Song, S.; Kosciolek, T.; Bokulich, N. A.; Lefler, J.; Brislawn, C. J.; Humphrey, G.; Owens, S. M.; Hampton-Marcell, J.; Berg-Lyons, D.; McKenzie, V.; Fierer, N.; Fuhrman, J. A.; Clauset, A.; Stevens, R. L.; Shade, A.; Pollard, K. S.; Goodwin, K. D.; Jansson, J. K.; Gilbert, J. A.; Knight, R. The Earth Microbiome Project Consortium. A communal catalogue reveals Earth's multiscale microbial diversity. *Nature* **2017**, *551* (7681), 457−463.

https://doi.org/10.1021/acs.est.3c09797
Environ. Sci. Technol. 2024, 58, 4167−4180

(79) Bolyen, E.; Rideout, J. R.; Dillon, M. R.; Bokulich, N. A.; Abnet, C. C.; Al-Ghalith, G. A.; Alexander, H.; Alm, E. J.; Arumugam, M.; Asnicar, F.; Bai, Y.; Bisanz, J. E.; Bittinger, K.; Brejnrod, A.; Brislawn, C. J.; Brown, C. T.; Callahan, B. J.; Caraballo-Rodríguez, A. M.; Chase, J.; Cope, E. K.; Da Silva, R.; Diener, C.; Dorrestein, P. C.; Douglas, G. M.; Durall, D. M.; Duvallet, C.; Edwardson, C. F.; Ernst, M.; Estaki, M.; Fouquier, J.; Gauglitz, J. M.; Gibbons, S. M.; Gibson, D. L.; Gonzalez, A.; Gorlick, K.; Guo, J.; Hillmann, B.; Holmes, S.; Holste, H.; Huttenhower, C.; Huttley, G. A.; Janssen, S.; Jarmusch, A. K.; Jiang, L.; Kaehler, B. D.; Kang, K. B.; Keefe, C. R.; Keim, P.; Kelley, S. T.; Knights, D.; Koester, I.; Kosciolek, T.; Kreps, J.; Langille, M. G. I.; Lee, J.; Ley, R.; Liu, Y.; Loftfield, E.; Lozupone, C.; Maher, M.; Marotz, C.; Martin, B. D.; McDonald, D.; McIver, L. J.; Melnik, A. V.; Metcalf, J. L.; Morgan, S. C.; Morton, J. T.; Naimey, A. T.; Navas-Molina, J. A.; Nothias, L. F.; Orchanian, S. B.; Pearson, T.; Peoples, S. L.; Petras, D.; Preuss, M. L.; Pruesse, E.; Rasmussen, L. B.; Rivers, A.; Robeson, M. S.; Rosenthal, P.; Segata, N.; Shaffer, M.; Shiffer, A.; Sinha, R.; Song, S. J.; Spear, J. R.; Swafford, A. D.; Thompson, L. R.; Torres, P. J.; Trinh, P.; Tripathi, A.; Turnbaugh, P. J.; Ul-Hasan, S.; Van Der Hooft, J. J. J.; Vargas, F.; Vázquez-Baeza, Y.; Vogtmann, E.; Von Hippel, M.; Walters, W.; Wan, Y.; Wang, M.; Warren, J.; Weber, K. C.; Williamson, C. H. D.; Wllis, A. D.; Xu, Z. Z.; Zaneveld, J. R.; Zhang, Y.; Zhu, Q.; Knight, R.; Caporaso, J. G. Reproducible, interactive, scalable and extensible microbiome data science using QIIME 2. *Nat. Biotechnol.* **2019**, *37* (8), 852−857.
(80) Callahan, B. J.; McMurdie, P. J.; Rosen, M. J.; Han, A. W.; Johnson, A. J. A.; Holmes, S. P. DADA2: High-resolution sample inference from Illumina amplicon data. *Nat. Methods* **2016**, *13* (7), 581−583.
(81) Quast, C.; Pruesse, E.; Yilmaz, P.; Gerken, J.; Schweer, T.; Yarza, P.; Peplies, J.; Glöckner, F. O. The SILVA ribosomal RNA gene database project: Improved data processing and web-based tools. *Nucleic Acids Res.* **2013**, *41*, 590−596.
(82) Bokulich, N. A.; Kaehler, B. D.; Rideout, J. R.; Dillon, M.; Bolyen, E.; Knight, R.; Huttley, G. A.; Gregory Caporaso, J. Optimizing taxonomic classification of marker-gene amplicon sequences with QIIME 2's q2-feature-classifier plugin. *Microbiome* **2018**, *6* (1), 1−17.
(83) Robeson, M. S.; O'Rourke, D. R.; Kaehler, B. D.; Ziemski, M.; Dillon, M. R.; Foster, J. T.; Bokulich, N. A.; Pertea, M. RESCRIPt: Reproducible sequence taxonomy reference database management. *PloS Comput. Biol.* **2021**, *17* (11), 1−37.
(84) Nilsson, R. H.; Larsson, K.-H.; Taylor, A. F. S.; Bengtsson-Palme, J.; Jeppesen, T. S.; Schigel, D.; Kennedy, P.; Picard, K.; Glöckner, F. O.; Tedersoo, L.; Saar, I.; Kõljalg, U.; Abarenkov, K. The UNITE database for molecular identification of fungi: Handling dark taxa and parallel taxonomic classifications. *Nucleic Acids Res.* **2019**, *47*, D259−D264.
(85) Kõljalg, U.; Nilsson, H. R.; Schigel, D.; Tedersoo, L.; Larsson, K.-H.; May, T. W.; Taylor, A. F. S.; Jeppesen, T. S.; Frøslev, T. G.; Lindahl, B. D.; Põldmaa, K.; Saar, I.; Suija, A.; Savchenko, A.; Yatsiuk, I.; Adojaan, K.; Ivanov, F.; Piirmann, T.; Pöhönen, R.; Zirk, A.; Abarenkov, K. The Taxon Hypothesis Paradigm—On the Unambiguous Detection and Communication of Taxa. *Microorganisms* **2020**, *8* (12), 1910.
(86) Nguyen, N. H.; Song, Z.; Bates, S. T.; Branco, S.; Tedersoo, L.; Menke, J.; Schilling, J. S.; Kennedy, P. G. FUNGuild: An open annotation tool for parsing fungal community datasets by ecological guild. *Fungal Ecol.* **2016**, *20*, 241−248.
(87) Team, R. C. R: A Language And Environment For Statistical Computing; R Foundation for Statistical Computing: Vienna, Austria, 2021 https://www.R-project.org/.
(88) Kassambara, A. ggpubr:'ggplot2' Based Publication Ready Plots. R package version 0.6.0, 2023 https://rpkgs.datanovia.com/ggpubr/.
(89) Anderson, M. J. A new method for non-parametric multivariate analysis of variance. *Austral Ecol.* **2001**, *26* (1), 32−46.
(90) Oksanen, J.; Simpson, G. L.; Blanchet, F. G.; Kindt, R.; Legendre, P.; Minchin, P. R.; O'Hara, R. B.; Solymos, P.; Stevens, M. H. H.; Szoecs, E.; Wagner, H.; Barbour, M.; Bedward, M.; Bolker, B.; Borcard, D.; Carvalho, G.; Chirico, M.; De Caceres, M.; Durand, S.; Evangelista, H. B. A.; FitzJohn, R.; Friendly, M.; Furneaux, B.; Hannigan, G.; Hill, M. O.; Lahti, L.; McGlinn, D.; Ouelletee, M.; Cunha, E. R.; Smith, T.; Stier, A.; Ter Braak, C. J. F.; Weedon, J. vegan: Community Ecology Package. R package version 2.5−7. 2020, 2022.
(91) Lu, Y.; Zhou, G.; Ewald, J.; Pang, Z.; Shiri, T.; Xia, J. MicrobiomeAnalyst 2.0: Comprehensive statistical, functional and integrative analysis of microbiome data. *Nucleic Acids Res.* **2023**, *51* (W1), W310−W318.
(92) Wickham, H. *Ggplot2: Elegant graphics for data analysis*, 2nd ed.; Springer International Publishing, 2016.
(93) Glaser, B.; Haumaier, L.; Guggenberger, G.; Zech, W. Black carbon in soils: The use of benzenecarboxylic acids as specific markers. *Org. Geochem.* **1998**, *29*, 811−819.
(94) Wiedemeier, D. B.; Hilf, M. D.; Smittenberg, R. H.; Haberle, S. G.; Schmidt, M. W. I. Improved assessment of pyrogenic carbon quantity and quality in environmental samples by high-performance liquid chromatography. *J. Chromatography. A* **2013**, *1304*, 246−250.
(95) Pulido-Chavez, M. F.; Alvarado, E. C.; DeLuca, T. H.; Edmonds, R. L.; Glassman, S. I. High-severity wildfire reduces richness and alters composition of ectomycorrhizal fungi in low-severity adapted ponderosa pine forests. *For. Ecol. Manage.* **2021**, *485*, 118923.
(96) Ferrenberg, S.; O'Neill, S. P.; Knelman, J. E.; Todd, B.; Duggan, S.; Bradley, D.; Robinson, T.; Schmidt, S. K.; Townsend, A. R.; Williams, M. W.; Cleveland, C. C.; Melbourne, B. A.; Jiang, L.; Nemergut, D. R. Changes in assembly processes in soil bacterial communities following a wildfire disturbance. *Isme J.* **2013**, *7* (6), 1102−1111.
(97) Najar, I. N.; Thakur, N. A systematic review of the genera Geobacillus and Parageobacillus: Their evolution, current taxonomic status and major applications. *Microbiology* **2020**, *166* (9), 800−816.
(98) Tong, D. Q.; Gill, T. E.; Sprigg, W. A.; Van Pelt, R. S.; Baklanov, A. A.; Barker, B. M.; Bell, J. E.; Castillo, J.; Gassó, S.; Gaston, C. J.; Griffin, D. W.; Huneeus, N.; Kahn, R. A.; Kuciauskas, A. P.; Ladino, L. A.; Li, J.; Mayol-Bracero, O. L.; McCotter, O. Z.; Méndez-Lázaro, P. A.; Mudu, P.; Nickovic, S.; Oyarzun, D.; Prospero, J.; Raga, G. B.; Raysoni, A. U.; Ren, L.; Sarafoglou, N.; Sealy, A.; Sun, Z.; Vimic, A. V. Health and Safety Effects of Airborne Soil Dust in the Americas and Beyond. *Rev. Geophys.* **2023**, *61* (2), 1−52.
(99) Santos, F.; Russell, D.; Berhe, A. A. Thermal alteration of water extractable organic matter in climosequence soils from the Sierra Nevada, California. *J. Geophys. Res.: Biogeosci.* **2016**, *121* (11), 2877−2885.
(100) Jian, M.; Berhe, A. A.; Berli, M.; Ghezzehei, T. A. Vulnerability of Physically Protected Soil Organic Carbon to Loss Under Low Severity Fires. *Front. Environ. Sci.* **2018**, *6*, 66.
(101) Ferreira, E. A.; Pacheco, C. C.; Rodrigues, J. S.; Pinto, F.; Lamosa, P.; Fuente, D.; Urchueguía, J.; Tamagnini, P. Heterologous Production of Glycine Betaine Using Synechocystis sp. PCC 6803-Based Chassis Lacking Native Compatible Solutes. *Front. Bioeng. Biotechnol.* **2022**, *9*, 1−19.
(102) Caldas, T.; Demont-Caulet, N.; Ghazi, A.; Richarme, G. Thermoprotection by glycine betaine and choline. *Microbiology* **1999**, *145* (9), 2543−2548.
(103) Donhauser, J.; Qi, W.; Bergk-Pinto, B.; Frey, B. High temperatures enhance the microbial genetic potential to recycle C and N from necromass in high-mountain soils. *Global Change Biol.* **2021**, *27* (7), 1365−1386.
(104) Brochier-Armanet, C.; Boussau, B.; Gribaldo, S.; Forterre, P. Mesophilic crenarchaeota: Proposal for a third archaeal phylum, the Thaumarchaeota. *Nat. Rev. Microbiol.* **2008**, *6* (3), 245−252.
(105) Kerou, M.; Schleper, C. Nitrososphaeraceae. In *Bergey's Manual of Systematics of Archaea and Bacteria*, 1st ed.; Whitman, W. B.; Rainey, F.; Kämpfer, P.; Trujillo, M.; Chun, J.; DeVos, P.; Hedlund, B.; Dedysh, S. Eds.; Wiley, 2016; pp. 12. DOI: .
(106) Yeager, C. M.; Northup, D. E.; Grow, C. C.; Barns, S. M.; Kuske, C. R. Changes in Nitrogen-Fixing and Ammonia-Oxidizing

https://doi.org/10.1021/acs.est.3c09797
Environ. Sci. Technol. 2024, 58, 4167−4180

Bacterial Communities in Soil of a Mixed Conifer Forest after Wildfire. *Appl. Environ. Microbiol.* **2005**, *71* (5), 2713−2722.
(107) Baldrian, P. Forest microbiome: Diversity, complexity and dynamics. *FEMS Microbiol. Rev.* **2017**, *41*, 109−130.
(108) Teira, E.; Van Aken, H.; Veth, C.; Herndl, G. J. Archaeal uptake of enantiomeric amino acids in the meso- and bathypelagic waters of the North Atlantic. *Limnol. Oceanogr.* **2006**, *51* (1), 60−69.
(109) Hallam, S. J.; Mincer, T. J.; Schleper, C.; Preston, C. M.; Roberts, K.; Richardson, P. M.; Delong, E. F. Pathways of Carbon Assimilation and Ammonia Oxidation Suggested by Environmental Genomic Analyses of Marine Crenarchaeota. *PloS Biol.* **2006**, *4* (4), No. e95.
(110) Tourna, M.; Stieglmeier, M.; Spang, A.; Könneke, M.; Schintlmeister, A.; Urich, T.; Engel, M.; Schloter, M.; Wagner, M.; Richter, A.; Schleper, C. *Nitrososphaera viennensis*, an ammonia oxidizing archaeon from soil. *Proc. Natl. Acad. Sci. U. S. A.* **2011**, *108* (20), 8420−8425.
(111) Nelson, D. C.; Flematti, G. R.; Ghisalberti, E. L.; Dixon, K. W.; Smith, S. M. Regulation of Seed Germination and Seedling Growth by Chemical Signals from Burning Vegetation. *Annu. Rev. Plant Biol.* **2012**, *63* (1), 107−130.
(112) Nelson, D. C.; Riseborough, J.-A. M.; Flematti, G. R.; Stevens, J. C.; Ghisalberti, E. L.; Dixon, K. W.; Smith, S. M. Karrikins Discovered in Smoke Trigger Arabidopsis Seed Germination by a Mechanism Requiring Gibberellic Acid Synthesis and Light. *Plant Physiol.* **2009**, *149* (2), 863−873.
(113) Battin, T. J.; Kaplan, L. A.; Findlay, S.; Hopkinson, C. S.; Marti, E.; Packman, A. I.; Newbold, J. D.; Sabater, F. Biophysical controls on organic carbon fluxes in fluvial networks. *Nat. Geosci.* **2008**, *1* (2), 95−100.
(114) Averill, C.; Waring, B. Nitrogen limitation of decomposition and decay: How can it occur? *Global Change Biol.* **2018**, *24* (4), 1417−1427.
(115) Laszakovits, J. R.; Mackay, A. A. Data-Based Chemical Class Regions for Van Krevelen Diagrams. *J. Am. Soc. Mass Spectrom.* **2022**, *33*, 198−202.
(116) Maranon-Jimenez, S.; Castro, J.; Kowalski, A. S.; Serrano-Ortiz, P.; Reverter, B. R.; Sanchez-Canete, E. P.; Zamora, R. Post-fire soil respiration in relation to burnt wood management in a Mediterranean mountain ecosystem. *For. Ecol. Manage.* **2011**, *261*, 1436−1447.
(117) Johnson, D. B.; Woolet, J.; Yedinak, K. M.; Whitman, T. Experimentally determined traits shape bacterial community composition one and five years following wildfire. *Nat. Ecol. Evol.* **2023**, *7* (9), 1419−1431.
(118) Mataix-Solera, J.; Cerda, A.; Arcenegui, V.; Jordan, A.; Zavala, L. M. Fire effects on soil aggregation: A review. *Earth Sci. Rev.* **2011**, *109*, 44−60.
(119) Soto, B.; Benito, E.; Diaz-Fierros, F. Heat-Induced Degradation Processes in Forest Soils. *Int. J. Wildland Fire* **1991**, *3*, 147−152.
(120) Kemper, W. D.; Rosenau, R. C. Aggregate stability and size distribution. In *Methods of Soil Analysis, Part 1. American Society of Agronomy*; Klute, A., Ed.; Wiley: Madison, Wisconsin, 2018; pp. 425442. DOI: .
(121) García-Corona, R.; Benito, E.; de Blas, E.; Varela, M. E. Effects of heating on some soil physical properties related to its hydrological behaviour in two north-western Spanish soils. *Int. J. Wildland Fire* **2004**, *13*, 195−199.
(122) Jian, M.; Berli, M.; Ghezzehei, T. A. Soil Structural Degradation During Low-Severity Burns. *Geophys. Res. Lett.* **2018**, *45* (11), 5553−5561.
(123) Pulido-Chavez, M. F.; Randolph, J. W. J.; Zalman, C.; Larios, L.; Homyak, P. M.; Glassman, S. I. Rapid bacterial and fungal successional dynamics in first year after chaparral wildfire. *Mol. Ecol.* **2023**, *32* (7), 1685−1707.

https://doi.org/10.1021/acs.est.3c09797
Environ. Sci. Technol. 2024, 58, 4167−4180